Hindawi Publishing Corporation
Journal of Nanomaterials
Volume 2013, Article ID 826471, 7 pages
http://dx.doi.org/10.1155/2013/826471

Research Article

Triple-Component Drug-Loaded Nanocomposites Prepared Using a Modified Coaxial Electrospinning

Wei Qian,[1] Deng-Guang Yu,[1] Ying Li,[1] Xiao-Yan Li,[1] Yao-Zu Liao,[2] and Xia Wang[1]

[1] *School of Materials Science & Engineering, University of Shanghai for Science and Technology, 516 Jungong Road, Yangpu District, Shanghai 200093, China*
[2] *School of Chemistry, University of Bristol, Bristol BS8 1TS, UK*

Correspondence should be addressed to Deng-Guang Yu; ydg017@usst.edu.cn and Xia Wang; wangxia@163.com

Received 17 June 2013; Accepted 27 November 2013

Academic Editor: Gaurav Mago

Copyright © 2013 Wei Qian et al. This is an open access article distributed under the Creative Commons Attribution License, which permits unrestricted use, distribution, and reproduction in any medium, provided the original work is properly cited.

Triple-component nanocomposites for improved sustained drug release profiles are successfully fabricated through a modified coaxial electrospinning process, in which only organic solvent N,N-dimethylacetamide was used as sheath fluid. Using polyacrylonitrile (PAN) as filament-forming matrix, ibuprofen (IBU) as functional ingredient, and polyvinylpyrrolidone (PVP) as the additional component, the IBU/PVP/PAN triple-component nanocomposites had uniform structure and an average diameter of 620 ± 120 nm and 650 ± 120 nm when the contents of PVP in the nanofibers were 10.5% and 22.7%, respectively. The optimal sheath-to-core flow rate ratio was 0.11 under a total sheath and core fluid flow rate of 1.0 mL/h. Compared with the IBU/PAN composite nanofibers, the triple-component composites could release 92.1% and 97.8% of the contained IBU, significantly larger than a value of 73.4% from the former. The inclusion of PVP in the IBU/PAN could effectively avoid the entrapment of IBU in the insoluble PAN molecules, facilitating the *in vitro* release of IBU. The modified coaxial process and the resulted multiple component nanocomposites would provide new way for developing novel drug sustained materials and transdermal drug delivery systems.

1. Introduction

Electrospinning is a one-step straightforward nanofiber fabrication process, in which electrical energy is exploited to dry and solidify microfluid jets directly [1–4]. The processes produce nanosized fibers very rapidly, often at approximately 10^{-2} s. As a result, the physical state of the components in the liquid solutions is often propagated into the solid nanofibers to generate solid dispersions at a molecular scale or polymer-based composites, with few discerned nanoparticles resulted from phase separation [5, 6]. There exist numerous reports of electrospinning being used to produce polymer-based nanocomposite in the form of nanofibers. By virtue of the advantageous properties of nanofibers (e.g., high surface area, high porosity, and continuous web structure), these composites usually display improved functional performance [7–11].

Significant progress has been made in this process throughout the past few years and electrospinning has advanced its applications in many fields, including pharmaceutics. Electrospun nanofibers show great promise for developing many types of novel drug delivery systems (DDS) due to their special characteristics and the simple but useful and effective top-down fabricating process. For controlled release of active pharmaceutical ingredients, electrospun nanofibers are reported to provide a series of controlled drug release profiles, such as immediate, pulsatile, delayed, sustained, and biphasic releases [12, 13]. Among them, sustained drug release is gaining considerable attention as a method of administering and maintaining desired drug concentrations in the blood within a specified therapeutic window, or in target tissues within a desired duration of drug delivery [14, 15]. The first study on the application of electrospun nanofibers in pharmaceutics focused on the sustained release of tetracycline hydrochloride

using poly(lactic acid) and poly(ethylene-co-vinyl acetate), as well as their blend as filament-forming polymeric matrices [16].

It has been broadly reported that drug-loaded nanofibers are fabricated through electrospinning of a codissolving solution of a guest pharmaceutical active ingredient and a host polymer. For these nanofibers, the initial burst effect is inevitable because of the large nanofiber surfaces, drug distribution on the nanofiber surfaces, and also the amorphous status of the drug. Yu et al. has reported a modified coaxial electrospinning process, by which a blank polymer layer was coated on the nanofibers to offer a zero-order drug release profile [14, 15]. However, there is still another problem waiting to be solved for electrospun two-component composites for providing fine sustained drug release profiles. The problem is that the encapsulated drug in the nanofibers was often not completely released into the dissolution medium owing to the entrapment of drug molecules by the filament-forming polymer molecules or gave an undesirable long time period of "leveling-off" release processes [17]. This phenomenon is even severe when the polymer matrix is insoluble and nondegradable, in which only about 70% of the contained drug could be effectively released out *in vitro* dissolution [17, 18].

Building on the previous discussion, this study investigates the addition of a third auxiliary component in the electrospun drug-loaded nanofibers, by which the drug release profiles can be efficaciously improved. Polyacrylonitrile (PAN) and ibuprofen (IBU) were selected as the model filament-forming matrix and drug, respectively. Polyvinylpyrrolidone (PVP), a hydrophilic polymer, was selected as the additional third component. Polyacrylonitrile (PAN) is a synthetic, semicrystalline organic polymer resin, with the linear formula $(C_3H_3N)_n$. It is a versatile polymer used to produce large variety of products including ultrafiltration membranes, hollow fibers for reverse osmosis, fibers for textiles, oxidized flame retardant fibers, carbon fiber, and medicated nanofibers [19]. For biomedical applications, PAN has been exploited as filament-forming matrix to generate medicated fibers through traditional wet-spinning, dry-spinning [20, 21], and also electrospinning [22]. However, the drug release profiles of drug-loaded PAN fibers are unsatisfied due to poor drug controlled release property [20–22]. A modified coaxial electrospinning process, characterized by an unspinnable solvent as sheath fluid, was exploited to generate the triple-component nanocomposites. This process has been used to realize several new possibilities, such as controlling the size of nanoparticles self-assembled from electrospun nanofibers, preparing ultrafine structures from concentrated polymer solutions previously thought unspinnable, improving systematically polymer nanofiber quality, and generating high quality carbon nanofiber precursors [12–15].

2. Experimental

2.1. Materials. PAN powders ($\overline{M}_w$ = 80,000) were provided by Jinshan Petrochemistry Co., Ltd. (Shanghai, China). PVP K30 ($\overline{M}_w$ = 58,000) was obtained from Shanghai Yunhong Pharmaceutical Aids and Technology Co., Ltd. (Shanghai, China). IBU was purchased from Wuhan Fortuna Chemical Co., Ltd. (Hubei, China). Methylene blue, N, N-dimethylacetamide (DMAc) were obtained from the Sinopharm Chemical Reagent Co., Ltd. (Shanghai, China). All reagents were analytical grade and were used without further purification. Water was double distilled just before use.

2.2. Modified Coaxial Electrospinning. The three types of core electrospinnable PAN solutions were prepared by first dissolving 15.0 g of PAN and 2 g of IBU in 100 mL DMAc, and then 0, 2, and 5 g PVP K30 were codissolved in them. For digital observation and optimization of sheath-to-core flow rate ratio, 5 ppm of methylene blue was added to the second solutions with a PVP content of 10.5% [$2/(15+2+2)\times 100\%$]. The sheath fluid was pure DMAc.

Two syringe pumps (KDS100 and KDS200, Cole-Parmer, IL, USA), a high-voltage power supply (ZGF 60 kV/2 mA, Shanghai Sute Corp., Shanghai, China), and a homemade concentric spinneret were used to conduct the electrospinning process. Following some optimizations, the applied voltage was fixed at 18 kV and the fibers were collected on an aluminum foil at a distance of 20 cm. All electrospinning processes were carried out under ambient conditions (24 ± 2°C; relative humidity, 57% ± 5%). The electrospinning process was recorded using a digital video recorder (PowerShot A490, Canon, Tokyo, Japan). The other parameters are listed in Table 1.

2.3. Characterization. The morphology of the nanofiber mats was assessed using a Quanta FEG450 scanning electron microscope (SEM) (FEI Corporation, The Netherlands). Prior to the examination, the samples were rendered electrically conductive by gold sputter coating under a nitrogen atmosphere. The average fiber diameter was determined by measuring their diameters in the FESEM images at more than 100 different locations using the Image J software (National Institutes of Health, MD, USA).

X-ray diffraction (XRD) patterns were obtained on a D/Max-BR diffractometer (RigaKu, Tokyo, Japan) with CuKα radiation within the 2θ range of 5°–60° at 40 mV and 30 mA. Differential scanning calorimetry (DSC) analyses were carried out using an MDSC 2910 differential scanning calorimeter (TA Instruments Co., New Castle, DE, USA). Sealed samples were heated at 10°C min^{-1} from 50 to 300°C under a nitrogen gas flow of 40 mL/min. Fourier transform infrared (FTIR) analyses were performed on a Nicolet-Nexus 670 FTIR spectrometer (Nicolet Instrument Corporation, WI, USA) from 500 cm^{-1} to 4000 cm^{-1} at a resolution of 2 cm^{-1}.

In vitro dissolution tests were carried out according to the Chinese Pharmacopoeia (2005 ed.) Method II, a paddle method in which an RCZ-8A dissolution apparatus (Tianjin University Radio Factory, Tianjin, China) was used. About 200 mg of drug-loaded nanofibers were placed in 900 mL of physiological saline (PS; 0.9 wt%) at 37 ± 1°C. The instrument was then set to 50 rpm, providing sink conditions in which $C < 0.2C_s$. At predetermined time points, 5.0 mL samples

Table 1: Parameters of the electrospinning processes and their products.

No.	Electrospinning	PVP content (%)	Flow rate (mL/h)			Morphology[b]	Diameter (nm)
			Sheath fluid[a]	Core fluid	Ratio		
F1	Single	10.5	0.0	1.0	0	Linear/thick fibers	780 ± 210
F2	Coaxial	10.5	0.1	0.9	0.11	Linear	620 ± 120
F3	Coaxial	10.5	0.2	0.8	0.25	Beads-on-a-string	440 ± 140
F4	Coaxial	0	0.1	0.9	0.11	Linear	610 ± 110
F5	Coaxial	22.7	0.1	0.9	0.11	Linear	650 ± 120

[a]Sheath fluid was DMAc.
[b]In this column, "linear" morphology refers to nanofibers with few beads or spindles on them.

were withdrawn from the dissolution medium and replaced with fresh medium to maintain a constant volume. After filtration through a 0.22 μm membrane (Millipore, MA, USA) and appropriate dilution with PS, the samples were analyzed at λ_{max} = 264 nm using a UV-vis spectrophotometer (UV-2102PC, Unico Instrument Co. Ltd., Shanghai, China). The cumulative amount of IBU released at each time point was reverse calculated from the data obtained against a predetermined calibration curve. Experiments were carried out six times and the results are presented as mean values.

3. Results and Discussion

3.1. The Modified Coaxial Electrospinning. A schematic diagram of the modified coaxial electrospinning process with solvent as sheath fluid is shown in Figure 1(a). A homemade concentric spinneret was used to carry out the modified process (Figure 1(b)). The critical voltage applied to a fluid to initiate Taylor cone formation and the straight thinning jet (V_c) have a close relationship with the diameter of sheath part of the concentric spinneret [12], as indicated by

$$V_c \sim \sqrt{\frac{\gamma d^2}{\varepsilon R}}, \quad (1)$$

where V_c is the critical voltage for a jet emanating from the meniscus tip, d is the electrode separation, ε is the permittivity, γ is the surface tension, and R is the principal curvature of the liquid meniscus. A small diameter of the spinneret's orifice means a big value of R, and thus a small V_c to imitate the coaxial electrospinning process. The homemade spinneret used in the study has an outer and inner diameter of 1.2 and 0.3 mm, respectively (Figure 1(b)), facilitating the coaxial electrospinning process. In addition, the inner capillary projects a little from the surface of the outer capillary, which is expected to make the sheath DMAc well encompass the core codissolving spinnable solutions.

When the modified coaxial electrospinning was carried out to prepare the composite nanofibers, two syringe pumps were used to drive the sheath and core fluids independently (Figure 2(a)). An alligator clip was used to connect the inner stainless steel capillary with the high voltage supply (Figure 2(b)). With DMAc as sheath fluid and under a sheath-to-core flow rate ratio of 0.11, the arrangement produced a typical fluid jet trajectory, in which a Taylor cone is followed by a straight fluid jet and a bending and whipping instability region (Figure 2(c)). As the applied voltage was boosted from 0 kV to 18 kV, the core-shell droplet was quickly transformed from a round shape (Figure 2(d)) to a cone shape, that is, the well-known Taylor cone (Figure 2(e)). The compound Taylor cone is clearly composed of two parts with the sheath solvent well surrounding the core polymer solutions, as indicated by the methylene blue in Figure 2(e). Although the modified coaxial process could not create core-sheath nanostructure, the surrounding solvent did facilitate a stable, continuous, and smooth electrospinning process, and it was expected to produce monolithic nanofibers with higher quality in terms of smaller diameters and smoother surfaces and with more uniform structures [23].

3.2. Morphology of the Nanofibers. In the modified coaxial electrospinning process, one of the most important parameters is the sheath-to-core flow rate ratio. To select a suitable value of the sheath flow rate, three different types of sheath-to-core flow rate ratios with a fixed total flow rate through the spinneret (1.0 mL/h, Table 1), that is, 0, 0.11, and 0.25, were taken to fabricate different triple-component nanofibers. Their FESEM images are shown in Figure 3. All the three kinds of nanofiber take linear structure. But when the electrospinning was carried out with a sheath flow rate of 0 (i.e., a single fluid electrospinning), very thick fibers (about several microns and a result of clogging of spinneret from time to time) exist in the nanofibers F1 (Figure 3(a)) although they have an average diameter of 780 ± 210 nm. When the sheath flow rate was increased to 0.25, there are many beads/spindles in the nanofibers (Figure 3(c)) although a thinner nanofiber with an average diameter of 440 ± 140 nm was achieved. In contrast, a suitable sheath-to-core flow rate ratio of 0.11 resulted in nanofibers with higher quality. The nanofibers F2 have smaller diameters and a narrower distribution of 620 ± 120 nm than F1 and a better linear structure than F3 (without any beads/spindles or very thick fibers within them). Based on these results, a sheath-to-core flow rate ratio of 0.11 was taken in the present study to generate nanofibers with different content of PVP in the IBU-loaded PAN nanofibers.

Shown in Figure 4 are FESEM images of nanofibers with different contents of PVP in them. All the three types of nanofibers have fine linear structure with few spindles or beads in them. With the increase of PVP in the nanofibers F4 (Figure 4(a)), F2 (Figure 4(b)), and F5 (Figure 4(c)), their

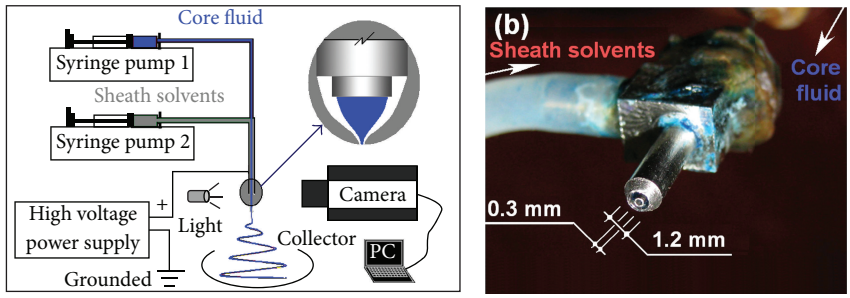

(a) (b)

FIGURE 1: A diagram of the modified coaxial electrospinning (a) and the concentric spinneret (b).

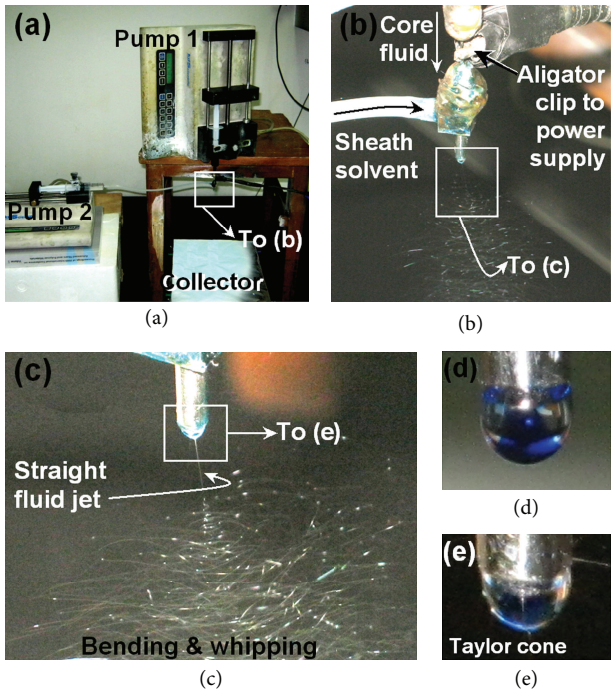

(a) (b) (c) (d) (e)

FIGURE 2: Observations of the modified coaxial electrospinning processes: (a) the arrangement of apparatus, (b) the connection of the concentric spinneret with the syringe pumps and the power supply, (c) a typical coaxial electrospinning process with DMAc as sheath fluid and under a sheath-to-core flow rate ratio of 0.11, (d) the core-shell droplet, and (e) the compound Taylor cone under an applied voltage of 18 kV.

average diameters were slightly increased from 610 ± 110 to 620 ± 120 and 650 ± 120 nm, respectively.

3.3. The Physical Status of the Components in the Nanofibers. The presence of numerous distinct peaks (Figure 5) in the X-ray diffraction patterns indicates that IBU was present as a crystalline material. The spectrum of amorphous PVP K30 was characterized by the complete absence of any diffraction peak. The PAN existed in a half-crystalline status, as demonstrated by the diffraction angle of 2θ at 16.71°. From Figure 5, it is clear that the characteristic diffraction peaks of IBU are completely absent for the three types of composite nanofibers. This result suggests that all the IBU in the double-component nanofibers F4 and triple-component composite nanofibers F2 and F5 was amorphous.

All DSC thermograms are shown in Figure 6. The DSC curve of pure IBU exhibited a single endothermic response corresponding to the melting point of IBU at 76°C (ΔH_f = −125 J/g). The profile for PAN did not demonstrate any fusion peak or phase transition before it decomposed at peak temperature around 300°C. As an amorphous polymer, PVP K30 did not show any fusion peaks but had a broad endotherm due to dehydration, which lies between 80°C and 120°C and with a peak at 86°C. PVP is a polymer and can be present in a glassy or rubber state. The change from one state to the other can be detected as a small glass transition around 160–180°C, as indicated by "A" in Figure 6 and also verified in the literature [24]. DSC thermograms of all the nanofibers (F2, F4, and F5) similarly did not give a melting peak of IBU and thus indicating that all incorporated drug was no longer present as a crystalline material. The results of DSC concurred with those of XRD that the original structure of IBU was lost and it was completely converted into an amorphous state in all the nanofibers regardless of one or two polymer matrices.

The FTIR spectra of PAN, PVP, IBU, and their composite nanofibers were shown in Figure 7. The existence of PAN in the composite nanofibers was confirmed by the typical absorption at 2243 cm^{-1} (–C≡N). By comparing the spectrum of IBU-loaded PAN nanofibers F4 and IBU-loaded PAN/PVP nanofibers F2 and F5, it is obvious that the IBU spectra has three typical peaks at 1570, 1610, and 1725 cm^{-1}, whereas all the nanofibers had only one peak at 1720 cm^{-1}. And all the peaks in the figure region of IBU spectra disappeared in the nanofibers' spectra. These results suggest that there are favorite secondary interactions among the components in the composite nanofibers. From the previously mentioned results and the molecular structure of IBU, PAN, and PVP, it can be speculated that in the double-component composite nanofibers of IBU/PAN, hydrogen bonding interactions may occur between IBU (–OH) and PAN (–C≡N), where IBU acted as H donor, and that in the triple-component composite nanofibers of F2 and F5, hydrogen bonding interactions could occur between IBU (–OH) and PAN (–C≡N) and also between IBU (–OH) and PVP (>C=O). These hydrogen bondings would take their role in keeping the IBU molecules evenly and stably distributed

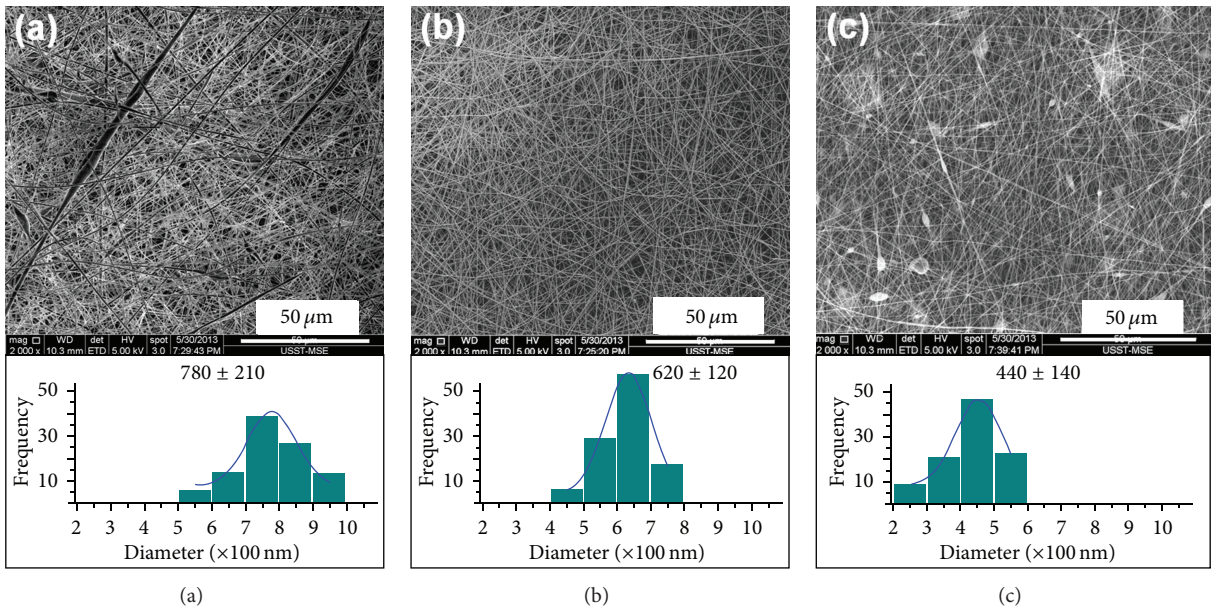

(a) (b) (c)

Figure 3: The FESEM images of nanofibers F1 (a), F2 (b), and F3 (c), which were generated under different sheath-to-core flow rate ratio of 0, 0.11, and 0.25, respectively. The total flow rate of sheath and core fluid was 1.0 mL/h.

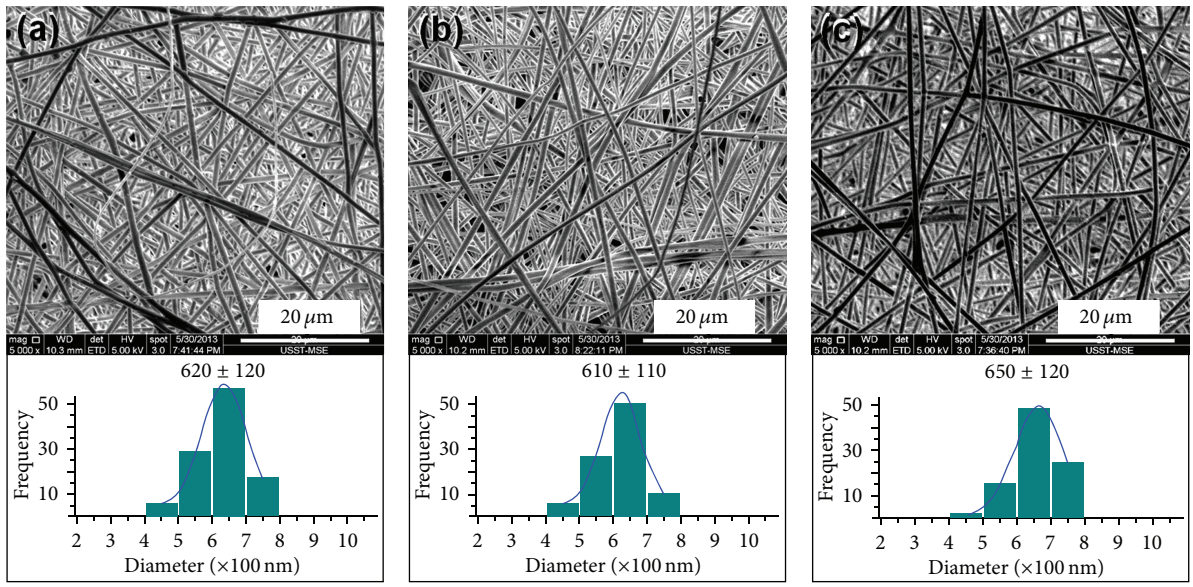

(a) (b) (c)

Figure 4: The FESEM images of nanofibers F2 (a), F4 (b), and F5 (c), which were generated under a sheath-to-core flow rate ratio of 0.11 and a total flow rate from the spinneret of 1.0 mL/h.

than in the double and triple-component nanofibers. Certainly, hydrophobic interactions could be speculated to be formed between PAN and PVP due to long carbon chains. Additionally, the typical peak of PAN at 2243 cm^{-1} gradually diminished with the content of PVP which increased from 0% to 22.7%, as indicated by the ellipse in Figure 7.

3.4. The In Vitro Drug Release Profiles. The *in vitro* release profiles of IBU from the composite nanofibers are shown in Figure 8. In the first hour, 36.3%, 35.7%, and 37.7% of the loaded IBU were released from the composite nanofibers F2, F4, and F5, respectively. The initial burst effect of the triple-components composite nanofibers F2 and F5 was slightly larger than that of double-component nanofibers, which should be attributed to the hydrophilic property and easy dissolution of PVP.

After 10 h *in vitro* dissolution tests, 83.7%, 68.3%, and 87.4% of the contained IBU was released into the dissolution medium for nanofibers F2, F4, and F5, respectively. And

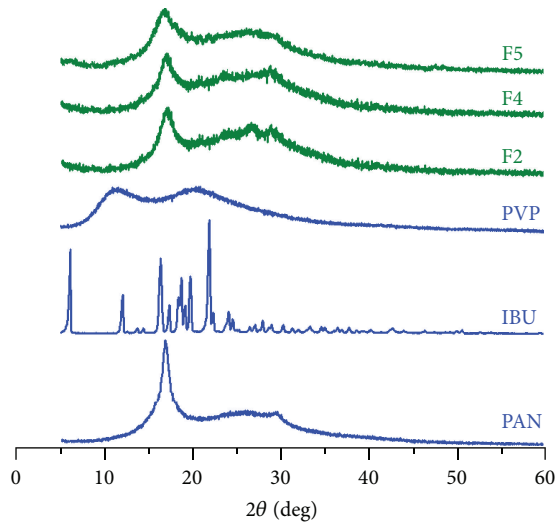

Figure 5: XRD patterns of the raw materials and their composite nanofibers.

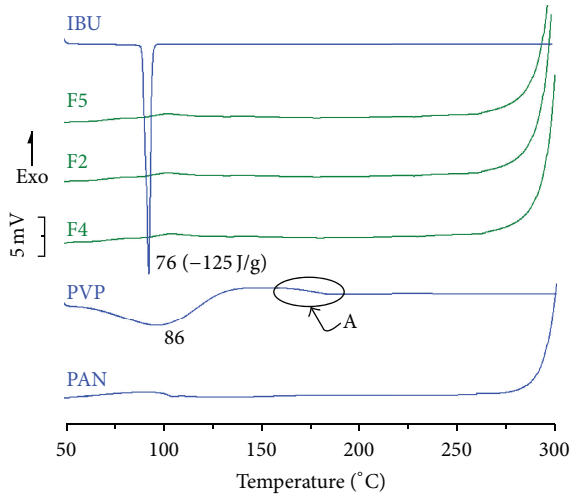

Figure 6: DSC thermograms of the components and their composite nanofibers.

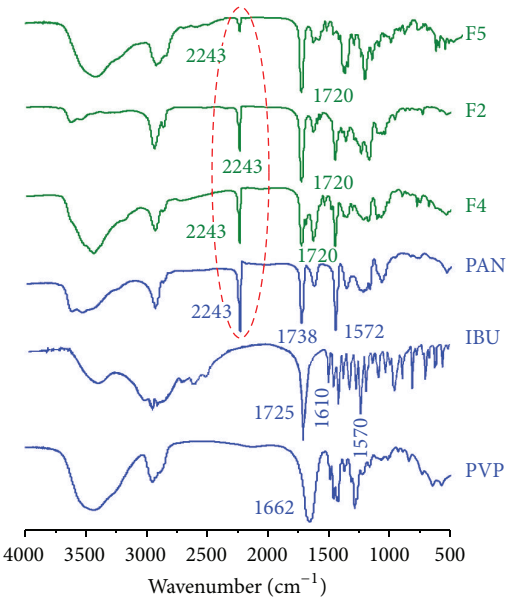

Figure 7: FTIR spectra of the raw materials and their composite nanofibers.

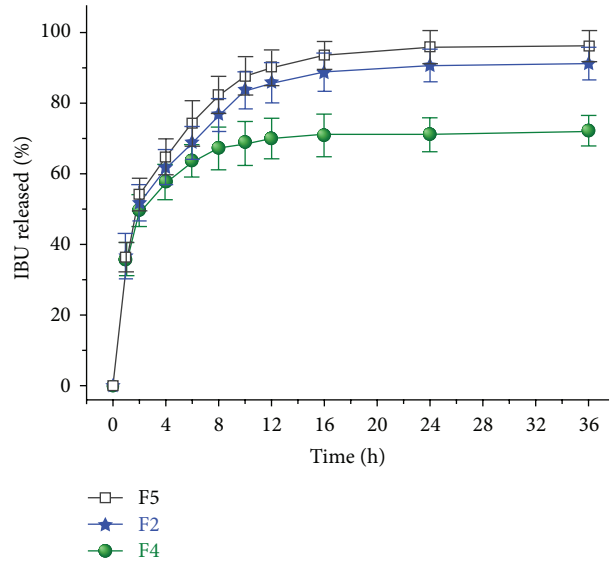

Figure 8: *In vitro* drug release profiles.

after 36 h *in vitro* dissolution tests, 92.1%, 73.4%, and 97.8% of the contained IBU were released out for nanofibers F2, F4, and F5, respectively. These results demonstrate that the triple-component composite nanofibers F2 and F5 have advantages over the double-component products F4 in that more active pharmaceutical ingredients can release out from the nanofibers during a certain time period. PVP not only is a hydrophilic polymer but also has good compatibility with the drug IBU (forming hydrogen bonding with IBU) and the electrospinning process (electrospinnable polymer) as well. During the *in vitro* dissolution processes, PVP could act as the pore-forming agent to form passages for the IBU entrapped in the inner part of the fibers to be gradually released out via diffusion mechanisms and thus facilitates the exhaustion process of loaded IBU from the fibers matrix and avoids the total entrapment in the insoluble PAN molecules.

4. Conclusions

This study experimented a new coaxial electrospinning process on smoothing the preparation of functional nanocomposites composed of multiple components. The sheath-to-core flow rate ratio is a key parameter for successfully carrying out the modified process and generating nanofibers with high quality. Under a condition of a sheath-to-core flow rate ratio of 0.11 and a sheath and core total fluid rate of 1.0 mL/h, IBU/PVP/PAN triple-component nanocomposites with uniform structure and an average diameter of 620 ± 120 nm and 650 ± 120 nm were created when the PVP contents were 10.5% and 22.7%, respectively. Compared

to the IBU/PAN double-component composites, the triple-component composites significantly improved the drug *in vitro* release profiles, efficaciously avoiding the entrapment of IBU in the insoluble PAN molecules in the IBU/PAN nanofibers. The modified coaxial process and the multiple-component nanocomposites would provide new ways for developing novel drug sustained materials and transdermal drug delivery systems.

Acknowledgments

This work was supported by the National Science Foundation of China (nos. 51373101, 51373100, and 51203090), the Natural Science Foundation of Shanghai (nos. 13ZR1428900 and 12ZR1446700), the Key Project of the Shanghai Municipal Education Commission (no. 13ZZ113), and the Innovation project of the University of Shanghai for Science and Technology (no. 13XGM01).

References

[1] T. Lin and X. Wang, *Encyclopedia of Nanoscience and Nanotechnology*, American Scientific, Los Angeles, Calif, USA, 2nd edition, 2011.

[2] L. Ji, Z. Lin, M. Alcoutlabi, and X. Zhang, "Recent developments in nanostructured anode materials for rechargeable lithium-ion batteries," *Energy and Environmental Science*, vol. 4, no. 8, pp. 2682–2689, 2011.

[3] X. Zhang, L. Ji, O. Toprakci, Y. Liang, and M. Alcoutlabi, "Electrospun nanofiber-based anodes, cathodes, and separators for advanced lithium-ion batteries," *Polymer Reviews*, vol. 51, no. 3, pp. 239–264, 2011.

[4] Y. Su, Q. Su, W. Liu et al., "Controlled release of bone morphogenetic protein 2 and dexamethasone loaded in core-shell PLLACL-collagen fibers for use in bone tissue engineering," *Acta Biomaterialia*, vol. 8, no. 2, pp. 763–771, 2012.

[5] D.-G. Yu, X.-X. Shen, C. Branford-White, K. White, L.-M. Zhu, and S. W. Annie Bligh, "Oral fast-dissolving drug delivery membranes prepared from electrospun polyvinylpyrrolidone ultrafine fibers," *Nanotechnology*, vol. 20, no. 5, Article ID 055104, 4 pages, 2009.

[6] X. Y. Li, X. Wang, D. G. Yu et al., "Electrospun Borneol-PVP nanocomposites," *Journal of Nanomaterials*, vol. 2012, Article ID 731382, 8 pages, 2012.

[7] L. Ji, Z. Lin, A. J. Medford, and X. Zhang, "In-situ encapsulation of nickel particles in electrospun carbon nanofibers and the resultant electrochemical performance," *Chemistry*, vol. 15, no. 41, pp. 10718–10722, 2009.

[8] H. Niu, J. Zhang, Z. Xie, X. Wang, and T. Lin, "Preparation, structure and supercapacitance of bonded carbon nanofiber electrode materials," *Carbon*, vol. 49, no. 7, pp. 2380–2388, 2011.

[9] L. Ji, Z. Lin, B. Guo, A. J. Medford, and X. Zhang, "Assembly of carbon-SnO_2 core-sheath composite nanofibers for superior lithium storage," *Chemistry*, vol. 16, no. 38, pp. 11543–11548, 2010.

[10] X. Wang, H. Niu, X. Wang, and T. Lin, "Needleless electrospinning of uniform nanofibers using spiral coil spinnerets," *Journal of Nanomaterials*, vol. 2012, Article ID 785920, 9 pages, 2012.

[11] H. Niu and T. Lin, "Fiber generators in needleless electrospinning," *Journal of Nanomaterials*, vol. 2012, Article ID 725950, 13 pages, 2012.

[12] D. G. Yu, G. R. Williams, X. Wang, X. K. Liu, H. L. Li, and S. W. A. Bligh, "Dual drug release nanocomposites prepared using a combination of electrospraying and electrospinning," *RSC Advances*, vol. 3, no. 14, pp. 4652–4658, 2013.

[13] D. G. Yu, X. Wang, X. Y. Li, W. Chian, Y. Li, and Y. Z. Liao, "Electrospun biphasic drug release polyvinylpyrrolidone/ethyl cellulose core/sheath nanofibers," *Acta Biomaterialia*, vol. 9, no. 3, pp. 5665–5672, 2013.

[14] D. G. Yu, X. Y. Li, X. Wang, W. Chian, Y. Z. Liao, and Y. Li, "Zero-order drug release cellulose acetate nanofibers prepared using coaxial electrospinning," *Cellulose*, vol. 20, no. 1, pp. 379–389, 2013.

[15] D. G. Yu, W. Chian, X. Wang, X. Y. Li, Y. Li, and Y. Z. Liao, "Linear drug release membrane prepared by a modified coaxial electrospinning process," *Journal of Membrane Sciences*, vol. 428, no. 3, pp. 150–156, 2013.

[16] E.-R. Kenawy, G. L. Bowlin, K. Mansfield et al., "Release of tetracycline hydrochloride from electrospun poly(ethylene-co-vinylacetate), poly(lactic acid), and a blend," *Journal of Controlled Release*, vol. 81, no. 1-2, pp. 57–64, 2002.

[17] D.-G. Yu, C. Branford-White, L. Li, X.-M. Wu, and L.-M. Zhu, "The compatibility of acyclovir with polyacrylonitrile in the electrospun drug-loaded nanofibers," *Journal of Applied Polymer Science*, vol. 117, no. 3, pp. 1509–1515, 2010.

[18] H.-M. Chen and D.-G. Yu, "An elevated temperature electrospinning process for preparing acyclovir-loaded PAN ultrafine fibers," *Journal of Materials Processing Technology*, vol. 210, no. 12, pp. 1551–1555, 2010.

[19] D.-G. Yu, P. Lu, C. Branford-White, J.-H. Yang, and X. Wang, "Polyacrylonitrile nanofibers prepared using coaxial electrospinning with LiCl solution as sheath fluid," *Nanotechnology*, vol. 22, no. 43, Article ID 435301, 7 pages, 2011.

[20] H.-L. Nie, Z.-H. Ma, Z.-X. Fan et al., "Polyacrylonitrile fibers efficiently loaded with tamoxifen citrate using wet-spinning from co-dissolving solution," *International Journal of Pharmaceutics*, vol. 373, no. 1-2, pp. 4–9, 2009.

[21] X. Shen, D. Yu, X. Zhang, C. Branford-White, and L. Zhu, "Preparation and characterization of TAM-loaded HPMC/PAN composite fibers for improving drug-release profiles," *Journal of Biomaterials Science*, vol. 22, no. 16, pp. 2227–2240, 2011.

[22] X. F. Zhang, D. G. Yu, S. J. Zhu, X. X. Shen, C. Branford-White, and L. M. Zhu, "Investigation of electrospun acyclovir-loaded ultrafine fiber mats," *Journal of Textiles Research*, vol. 30, no. 2, pp. 1–4, 2009.

[23] S. Agarwal, A. Greiner, and J. H. Wendorff, "Functional materials by electrospinning of polymers," *Progress in Polymer Science*, vol. 38, no. 2, pp. 963–991, 2013.

[24] D.-G. Yu, L.-D. Gao, K. White, C. Branford-White, W.-Y. Lu, and L.-M. Zhu, "Multicomponent amorphous nanofibers electrospun from hot aqueous solutions of a poorly soluble drug," *Pharmaceutical Research*, vol. 27, no. 11, pp. 2466–2477, 2010.

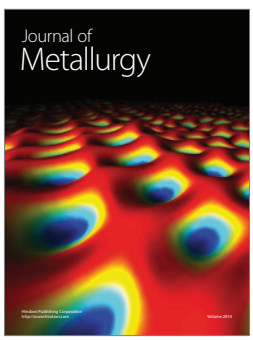

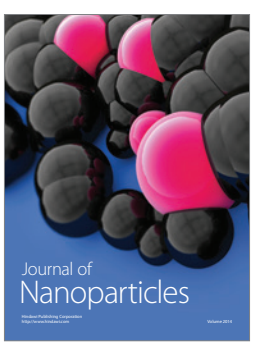

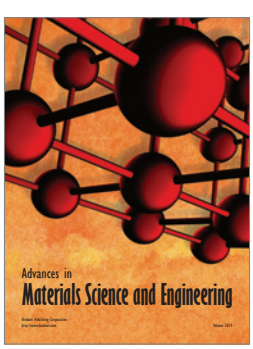

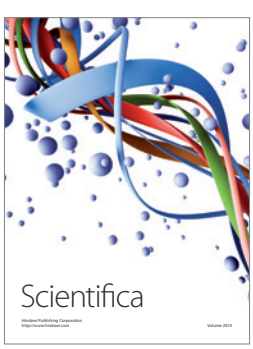

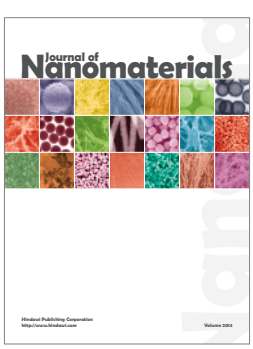

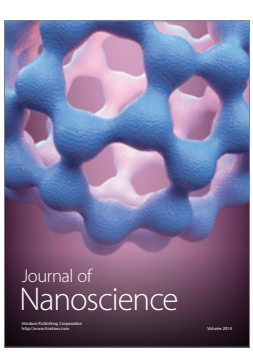

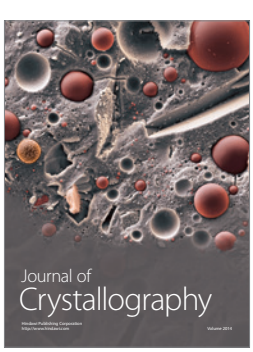

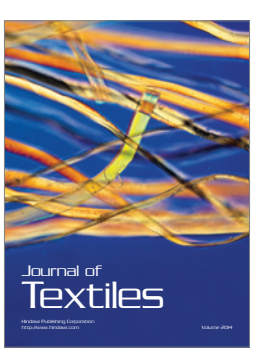

Hindawi

Submit your manuscripts at
http://www.hindawi.com